

RSK2 Protein Suppresses Integrin Activation and Fibronectin Matrix Assembly and Promotes Cell Migration*

Received for publication, October 9, 2012. Published, JBC Papers in Press, November 1, 2012, DOI 10.1074/jbc.M112.423046

Joanna E. Gawecka^{‡1}, Shirley S. Young-Robbins^{‡1}, Florian J. Sulzmaier^{‡§}, Maisel J. Caliva[‡], Minna M. Heikkilä[‡], Michelle L. Matter^{‡1,2}, and Joe W. Ramos^{‡§3}

From the [‡]Cancer Biology Program, University of Hawaii Cancer Center and the ¹Department of Cell and Molecular Biology, John A. Burns School of Medicine, University of Hawaii at Manoa, Honolulu, Hawaii 96813 and the [§]Department of Molecular Biosciences and Bioengineering, University of Hawaii at Manoa, Honolulu, Hawaii 96822

Background: RSK2 alters cell migration and metastasis, but the mechanism is incompletely understood.

Results: RSK2 inactivates integrins, increases filamin binding to integrin tails, alters actin distribution, increases migration, and decreases fibronectin matrix assembly.

Conclusion: RSK2 mediates inactivation of integrins and thus modulates integrin functions.

Significance: These findings provide a novel mechanism by which RSK2 affects migration and may lead to more selective ways to inhibit RSK2-dependent metastasis.

Modulation of integrin activation is important in many cellular functions including adhesion, migration, and assembly of the extracellular matrix. RSK2 functions downstream of Ras/Raf and promotes tumor cell motility and metastasis. We therefore investigated whether RSK2 affects integrin function. We report that RSK2 mediates Ras/Raf inactivation of integrins. As a result, we find that RSK2 impairs cell adhesion and integrin-mediated matrix assembly and promotes cell motility. Active RSK2 appears to affect integrins by reducing actin stress fibers and disrupting focal adhesions. Moreover, RSK2 co-localizes with the integrin activator talin and is present at integrin cytoplasmic tails. It is thereby in a position to modulate integrin activation and integrin-mediated migration. Activation of RSK2 promotes filamin phosphorylation and binding to integrins. We also find that RSK2 is activated in response to integrin ligation to fibronectin. Thus, RSK2 could participate in a feedback loop controlling integrin function. These results reveal RSK2 as a key regulator of integrin activity and provide a novel mechanism by which it may promote cell migration and cancer metastasis.

conformations: Bent-Closed (or low affinity), Extended-Closed (intermediate affinity), and Extended-Open (high affinity) (5). There are 18 distinct α -subunits and 8 β -subunits that can form up to 24 different heterodimers that interact with various extracellular matrix proteins.

Integrin activity and function is controlled by inside-out signaling. Several members of the Ras family of small GTPases regulate inside-out pathways that modulate integrin affinity. They activate or inactivate integrins depending on the GTPase involved and the cell type. For example in fibroblasts R-Ras activates integrins (6), whereas the related GTPase, H-Ras, suppresses activation of integrins in a transcription-independent manner (7). H-Ras also modulates integrin-mediated cell migration and fibronectin matrix assembly by initiating the Raf/ERK MAPK signaling cascade (6–9). The exact mechanism by which integrin activation is controlled continues to be an area of intense research focus. Although the mechanism of integrin activation by Rap through talin has been well worked out, the mechanism by which H-Ras inactivates integrins remains less clear. H-Ras suppresses integrin affinity for ligand via its downstream effector, the serine/threonine kinase Raf-1, in a transcription-independent manner (7). However, this suppression does not require activation of ERK1/2 MAP kinase, nor is it reversed by an inhibition of ERK1/2 activation (10). These results raise the question of whether Raf can activate ERK-independent pathways to inhibit integrin activation.

RSK2 is a substrate of ERK and mediates several of the biological functions of the Ras/MAP kinase pathway, such as regulation of cell cycle, differentiation, survival, and proliferation. The regulation of RSK activity is complex and requires phosphorylation at several sites by a variety of kinases in addition to autophosphorylation (11, 12). RSK has numerous substrates, including ones that affect cell motility, survival, proliferation, and growth (11, 13). RSK2 is overexpressed in both breast and prostate tumors and promotes proliferation in these cells (11, 14). It can also promote cell invasion and metastasis in head and neck cancers in addition to lung cancer in part through transcriptional mechanisms (13, 15, 16). However, the mechanisms

Changes in cell adhesion and migration are critical in cancer metastasis (1–3). Integrins are transmembrane heterodimeric receptors that not only mediate cell adhesion and motility but also transduce signaling that regulates cell proliferation, survival, and gene expression (1, 2, 4). Integrins consist of two noncovalently associated subunits, α and β , both of which contribute to the binding of ligand. They exist in at least three

* This work was supported, in whole or in part, by National Institutes of Health Grants R01-CA093849 and R01-GM088266 (to J. W. R.). This work was also supported by Grant 20061496 from the Robert C. Perry Fund of the Hawai'i Community Foundation (to J. W. R.) and Department of Defense Grant 05245002 (to J. W. R.).

⌘ Author's Choice—Final version full access.

¹ These authors contributed equally to this work.

² Supported by National Center for Research Resources Grant P20-RR016453.

³ To whom correspondence should be addressed: Cancer Biology Program, University of Hawaii Cancer Center, University of Hawaii at Manoa, 651 Iloilo St., Honolulu, HI 96813. Tel.: 808-564-5843; Fax: 808-587-0742; E-mail: jramos@cc.hawaii.edu.

underlying these functions are just beginning to be identified. RSK is clinically relevant in several human diseases, including cancer (17–19) and Coffin-Lowry syndrome (20). Several RSK-specific small molecule inhibitors are available that provide useful tools to better understand its function and determine its suitability as a target for clinical applications.

Integrin function is regulated by the association of a number of integrin-binding proteins that interact with the cytoplasmic tails. These include talin, filamin, and kindlins among others. Filamin A is an integrin- and actin-binding protein that serves as a scaffold for multiple proteins, including H-Ras, and may thereby mediate their signaling to integrins (21, 22). Alternatively, talin is another integrin and actin-binding cytoskeletal protein that mediates the final step in integrin activation (23–26). The kindlin family also appear to be required in some instances (27). Nevertheless the head domain of talin in isolation can activate a single integrin dimer, strongly supporting a direct role for talin in integrin activation (28). Interestingly, NMR studies revealed an autoinhibitory interaction between the talin rod and talin head domains that prevents it from binding to integrins (29). Thus, other proteins may be required to activate the release of the talin head domain from its autoinhibitory interaction with the talin rod domain and thereby activate integrins.

RSK2 functions downstream of Ras/Raf and can modulate cell migration and metastasis; we therefore investigated its role in the regulation of integrin activation and function. We report that RSK2 inactivates integrins and mediates Ras-dependent integrin suppression. The suppressive effect RSK2 has on integrin activation modulates integrin function. RSK2 impairs cell adhesion and integrin-mediated fibronectin matrix assembly and promotes cell motility. Active RSK2 appears to affect integrins by reducing actin stress fibers and disrupting focal adhesions. Furthermore, RSK2 co-localizes with talin and is present in a complex at integrin cytoplasmic tails. It is thereby in a position to modulate talin integrin activation and filamin effects on migration. Indeed, we show that RSK2 phosphorylates filamin and that this leads to increased filamin association with the integrin tails. The effect of RSK2 on filamin binding to integrins therefore corresponds to its effects on integrin activation. Moreover, RSK2 is activated in response to integrin ligation to fibronectin. This suggests that RSK2 could participate in a feedback loop controlling integrin adhesion and migration. Thus, RSK2 is a novel regulator of integrin activity downstream of Ras. RSK2 regulation of integrin activity may therefore contribute to its enhancement of tumor cell migration and metastasis. Hence, RSK2 signaling to integrins might provide novel drug targets in antimetastasis therapies.

EXPERIMENTAL PROCEDURES

Antibodies and Reagents

We obtained the antibodies described in this work from the following sources: RSK2 (Santa Cruz Biotechnology, sc-1430), p-RSK2 S227 (BIOSOURCE, A8172), p-RSK2 Y529 (Cell Signaling, 9324S), p-RSK2 S386 (BIOSOURCE, A8545), ERK (Santa Cruz Biotechnology, 93), p-ERK (Cell Signaling, 4370), Fibronectin (Santa Cruz Biotechnology, 9068), vimentin

(Sigma, V5225), filamin A (Cell Signaling, 4762; Abcam, ab51217), Ser(P)-2152-filamin A (Cell Signaling, 4761), actin (Santa Cruz Biotechnology, sc-1615), talin (Sigma, T3287), talin-head domain (Santa Cruz Biotechnology, 15336), HA-probe (Santa Cruz Biotechnology, sc-805), and tubulin (Santa Cruz Biotechnology, sc12462-R and sc-322293). The RSK inhibitors used are FMK (courtesy of J. Taunton, University of California San Francisco) and SL0101-1 (Tocris, 2250). The following cDNA constructs were also used where described: c-RafBXB-T481A (courtesy of M. White, University of Texas Southwestern), DA H-Ras (H-RasG12V) (courtesy of C. Der, University of North Carolina, Chapel Hill), HA-RSK2, DA-RSK2 (RSK2-Y707A), and DN-RSK2 (K100A) (courtesy of T. Sturgill, University of Virginia), integrin cytoplasmic tails (courtesy of M. Ginsberg, University of California San Diego), and HA-talin (courtesy of D. Calderwood, Yale University).

Cell Culture and Transfections

HeLa and CHOK1 cells were purchased from the American Type Culture Collection (Manassas, VA). Human prostate cancer cells (DU-145) were obtained from the DCTD Tumor Repository of the National Cancer Institute (Frederick, MD). Human mesothelioma cells (MILL) were a kind gift from Dr. H. Yang (University of Hawaii Cancer Center). HeLa, CHOK1, and MILL cell lines were cultured in DMEM containing L-glutamine (HyClone Thermo Scientific, Fair Lane, NJ) supplemented with 10% fetal bovine serum, nonessential amino acids, and antibiotics. DU-145 cells were cultured in RPMI supplemented with the additives mentioned above. Standard transient transfections for all cell lines were conducted using Genejuice (EMD Millipore), Lipofectamine 2000, or Lipofectamine (Invitrogen) according to the manufacturer's directions.

Lentiviral Knockdown of RSK2

RSK2 shRNA lentiviral particles (sc-36441-V) and control shRNA lentiviral particles (sc-108080) were obtained from Santa Cruz Biotechnology Inc. HeLa cells were plated in 12-well dishes 24 h prior to lentiviral infection. The cells were infected the following day with 100,000 infectious units of lentiviral particles/well in complete cell culture medium containing 5 μ g/ml Polybrene (Santa Cruz, sc-134220). The control shRNA lentiviral particles served as a scrambled negative control that will not lead to specific degradation of any cellular mRNA. 48 h post-infection, the cells were split 1:5 and selected for cells stably expressing shRNA for the knockdown of RSK2. Selection media contained 4 μ g/ml Puromycin dihydrochloride (Santa Cruz, sc-108071) and was replaced every other day. The cells were monitored for 14 days and then subjected to further experimental analysis. Knockdown of RSK2 was verified by immunoblotting.

Immunoblotting

The cells were lysed with ice-cold M2 lysis buffer (20 mM Tris-HCl, pH 7.6, 250 mM NaCl, 0.5% Nonidet P-40, 5 mM EDTA, 3 mM EGTA, 20 mM sodium phosphate, 20 mM sodium pyrophosphate, 3 mM β -glycerophosphate, 1 mM sodium orthovanadate, 1 mM phenylmethylsulfonyl fluoride) containing complete protease inhibitor mixture (11836153001; Roche

RSK2 Suppresses Integrin Activation

Applied Science). Cell lysates were cleared by centrifugation. Protein concentration was measured using the BCA assay kit (Pierce). Equal protein concentrations of cell lysates were resolved on SDS-PAGE. After electrophoresis, the proteins were transferred to PVDF (Millipore Corp., Bedford, MA) and immunoblotted. The membranes were blocked for 1 h with blocking buffer (5% milk with PBS-T) and then incubated with appropriate antibodies. The membranes were washed and incubated with horseradish peroxidase-conjugated secondary antibodies. Immunoblots were visualized by ECL (PerkinElmer Life Sciences). Alternatively, immunoblots were prepared with secondary antibodies conjugated to infrared fluorochromes and visualized via the Odyssey infrared imaging system (LI-COR Bioscience).

Integrin Activation and Flow Cytometry (PAC-1 and Fn9.11 Assays)

The activation state of endogenous $\beta 1$ integrin in response to transient transfection of the indicated cDNAs was assessed by three-color FACS assays as previously described (30, 31). Briefly, 24–48 h after transfection, the cells were harvested and analyzed for transfection efficiency (GFP) and the binding of chimeric $\alpha_{\text{IIB}}\alpha 6\beta 3\beta 1$ integrin to PAC-1 antibody (Becton Dickinson, 340535) (see Fig. 1, A and 1B) or integrin $\alpha 5\beta 1$ binding to 3FN-(9–11) fusion protein (see Fig. 1C). For each transfection, the harvested cells were divided into three tubes. The three preparations were used to assay for binding to ligand alone or binding in the presence of integrin inhibitor (Ro43 or 10 mM EDTA) or carried out in the presence of integrin activator (Ab33 or 10 mM MnCl_2). Activated integrins bound to PAC-1 or 3FN-(9–11) were detected with secondary antibodies conjugated to fluorochromes as indicated (eBioscience, 12-5990-1; Invitrogen, S868, respectively). All incubations and washes were carried out using $1\times$ Tyrode's buffer (10 mM HEPES, 10 g of NaCl, 1.015 g of NaHCO_3 , 0.195 g KCl, 1 mg/ml dextrose, 1 mg/ml bovine serum albumin, 1 mM CaCl_2 , 1 mM MgCl_2 , pH 7.4). Propidium iodine (1 ng/ μg) was added to each sample for the last 5 min. The samples were washed once before analysis. Gating was set such that only living (propidium iodine negative) cells expressing GFP were examined for PAC or 3FN-(9–11) binding. Integrin activation was quantified as an activation index, previously defined as $100 * (F - F_0)/(F_m - F_0)$, where F represents the geometric mean fluorescence of ligand binding alone, F_0 is the geometric mean fluorescence of ligand binding in the presence of inhibitor, and F_m is the geometric mean fluorescence of ligand binding in the presence of activator. Flow cytometry data analysis was done with FlowJo or BD CellQuest Pro FACS analysis software.

Cell Adhesion

An Immulon-2 96-well plate was precoated overnight with fibronectin or laminin as indicated. The uncoated sites on the plate were blocked with 2% heat-inactivated BSA for 2 h at room temperature, and the plate was washed with serum-free DMEM. Even numbers of cells were plated in $\sim 100 \mu\text{l}$ and incubated 1 h at 37 °C in tissue culture incubator. The wells then were washed with a low shear washing method until BSA-coated control wells did not have any adherent cells left. To

determine 100% of cells for quantification, some wells were not washed before fixing with glutaraldehyde for 20 min. For experimental cells, after the last wash, the cells were fixed in 100 μl of 2% glutaraldehyde (in PBS) for 10 min. The fixative was then aspirated, and the wells were air-dried for 5 min before incubation with 0.5% crystal violet solution for 45 min. The wells were then washed three times 200 μl of PBS and allowed to air dry. The cells were then solubilized in 100 μl of 10% acetic acid for 30 min. Signal development was examined at 560 nm by a UV-visible spectrophotometer.

Fibronectin Matrix Assembly

The cells were plated on glass coverslips and co-transfected with the indicated cDNA and GFP (as a transfection marker). 24 h after transfection, human plasma FN⁴ (100 $\mu\text{g}/\text{well}$) was added with the media and incubated for 24 h at 37 °C. The cultures were washed with $1\times$ PBS and fixed in 4% paraformaldehyde and 10 mM sucrose, pH 7.4, for 30 min at room temperature. The cells were incubated with 3% BSA/PBS for 30 min, stained with a polyclonal rabbit anti-human FN antibody (Santa Cruz Biotechnology) for 1 h, and washed three times in PBS, followed by goat anti-rabbit rhodamine-labeled IgG secondary antibody (Sigma-Aldrich). Coverslips were mounted with Fluormount-G mounting media and immunofluorescence analyzed using a Zeiss Axiovert 200M inverted microscope. Quantification of fibronectin matrix was determined as previously described (32, 33). Briefly, transfected cells were cultured in 6-well culture plates. After 24 h, the culture media was replaced with medium containing human FN (100 $\mu\text{g}/\text{ml}$). The cells were cultured for a further 35 h and washed twice with PBS, scraped into deoxycholate (DOC) buffer (1% sodium DOC, 2 mM *N*-ethylmaleimide, 2 mM iodoacetic acid [sodium salt], 2 mM EDTA, 2 mM PMSF, and 20 mM Tris-HCl, pH 8.5) on ice. Insoluble material was collected by centrifugation at 20,000 $\times g$ for 20 min at 4 °C. The DOC insoluble material was washed once in DOC buffer, resuspended in $5\times$ Tris-glycine SDS sample buffer, heated to 95 °C, and run on a Bis-Tris gel. After immunoblotting onto PVDF, the membranes were blocked (5% non-fat dry milk, 0.1% Tween 20 in $1\times$ PBS, pH 7.4) and probed with a human anti-FN antibody. Binding was visualized using the ECL system. The same membranes were re-probed with anti- α -tubulin antibody. Additionally, quantification of assembled matrix detected in the immunofluorescence study was performed using ImageJ WCIF image analysis software ($n = 6$).

Cell Migration Assays

Transwell Assay—The lower sides of Transwell filters (8.0- μm pore size; Costar) were coated overnight at 4 °C with 10 $\mu\text{g}/\text{ml}$ human plasma fibronectin. The cells were plated on the uncoated top side of the filters in incomplete DMEM, whereas the bottom chamber was filled with complete DMEM and 10 ng/ml EGF. The cells were incubated for the indicated time at 37 °C. The uncoated top side of each filter was then swabbed with a cotton tip applicator to remove cells that had not migrated through. The remaining cells were fixed with 2%

⁴ The abbreviations used are: FN, fibronectin; DOC, deoxycholate; FMK, fluoro-methyl ketone.

glutaraldehyde for 30 min. To detect β -galactosidase activity in only the transfected cells that had migrated through the filters, cells on the bottom side of each filter were stained overnight in 5-bromo-4-chloro-3-indolyl- β -D-galactopyranoside (X-gal) buffer overnight at 37 °C. Alternatively, migrated cells were stained with Calcein-AM (Sigma-Aldrich). After the assay incubation time, cell culture medium from the lower compartment was replaced with serum-free medium supplemented with 8 μ M Calcein-AM and incubated for 45 min at 37 °C. After the staining step, the cells were detached from the bottom side of the inserts by trypsinization. Migration was quantified by counting the β -galactosidase-stained cells under a bright field microscope or by measuring the fluorescence emission of Calcein-AM at 520 nm upon excitation at 485 nm with a fluorescence plate reader (PerkinElmer Life Sciences).

Scratch Assay—HeLa cells were transiently transfected with activated RSK2 or control vector. Alternatively, the cells were treated with FMK or control carrier. After 24 h, the cell monolayer was scratched with a micropipette tip. The closure of the scratch was followed using a Zeiss Axiovert 200M inverted microscope. The number of cells that migrated into the scratch within 24 h was counted under phase optics. The relative scratch filling rate was calculated as a ratio of the number of cells that migrated into the scratch to the number of migrating control cells.

Viability Assay

The cells were treated with 100 μ M SL0101-1, 20 μ M FMK, or carrier control for the time indicated and then subjected to a cell viability assay using the XTT cell proliferation kit (Roche Applied Science) according to the manufacturer's instructions. The cells were seeded at a concentration of 5×10^4 /well in a 96-well plate. Cultures were incubated at 37 °C in 50 μ l of XTT labeling mixture for 4 h. Absorbance of the samples at a wavelength of 492 nm was determined using an ELISA plate reader with a reference wavelength of 690 nm.

Immunofluorescence

The cells were plated on glass coverslips 24 h prior to transfection with the indicated cDNAs using Lipofectamine2000 (Invitrogen). 48 h after transfection, the cells were fixed with 4% paraformaldehyde, permeabilized, and blocked. The cells were then stained with the indicated antibodies. Actin was detected using a rhodamine phalloidin dye (Invitrogen). For talin detection, HeLa cells were lifted at 24 h post-transfection and allowed to re-adhere to coverslips coated with 10 μ g/ml fibronectin. Fluorescence microscopy was performed on a Zeiss Axiovert 200M with a 100 \times Oil objective. Confocal imaging was performed on a Leica TCS SP5 with 63 \times oil objective (Leica, Solms, Germany). Additionally, quantification of actin cytoskeleton rearrangement and focal adhesion formation detected in the immunofluorescence study was performed by a blind study and is presented as a percentage of cells showing an altered staining pattern ($n = 85$ for actin stained samples).

Integrin Tail Pulldowns

Recombinant, His-tagged human integrin cytoplasmic tail model proteins were produced and purified as previously

described (34, 35). Binding assays using recombinant integrin cytoplasmic tails bound to His-bind resin (Novagen) were performed as previously described (34, 35). Briefly, CHOK1 cells were transfected with the indicated DNA using Lipofectamine2000 (Invitrogen), and the cells were harvested 24–48 h later and lysed with XP lysis buffer. Cell lysates were incubated with integrin tails bound to beads for 24 h, washed, resuspended in SDS sample buffer, heated for 5 min at 95 °C, and analyzed for binding by SDS-PAGE. The lysate lanes in the immunoblotting images represent 2.5 or 5% input of total lysate protein amount mixed with the integrin tails and serve as references for the relative protein amounts used in the assay.

In Vitro Kinase Assays

In vitro kinase assays were performed as follows. Briefly, 10 μ g of substrate was incubated with 100 ng of active RSK2 (SignalChem), and 1.25 nmol of ATP in 1 \times kinase buffer (Cell Signaling) or 0.8 μ Ci/ μ l [γ - 32 P]ATP (PerkinElmer Life Sciences) with 1.25 nmol of ATP in 3 \times kinase buffer. The kinase reactions were carried out at 30 °C for 30 min and then terminated by addition of SDS sample buffer. Kinase substrates were prepared as follows: HA-talin (Santa Cruz HA[Y-11]) was immunoprecipitated from lysates prepared from CHOK1 cells that had been serum-starved (0.5% FBS) for 24 h. The complexes were precipitated by incubation with protein A/G-agarose beads (Santa Cruz), collected, and washed with radioimmune precipitation assay buffer. Wild-type and mutant filamin A (courtesy of John Blenis, Harvard University) were purified as GST fusion proteins from *Escherichia coli* (BL21[DES]) as previously described (36, 37).

Outside-in Signaling upon Integrin Binding to Ligand

Tissue culture plates were coated with 15 μ g/ml fibronectin for 24 h at 4 °C. CHOK1 cells were grown to confluence. The cells were lifted from the dish with nonenzymatic cell dissociation buffer (Invitrogen) and allowed to adhere to fibronectin-coated cell culture plates for 0 min, 5 min, 15 min, 30 min, 1 h, or 2 h. The cells were washed with 1 \times PBS and lysed with M2 lysis buffer. The cell lysates were cleared by centrifugation. Protein concentration was measured by BCA assay kit (Pierce). Cell lysates were resolved on SDS-PAGE and characterized by immunoblotting.

RESULTS

RSK2 Inhibits Integrin Activation and Impairs Cell Adhesion—H-Ras- and Raf-dependent inactivation of integrins does not require ERK1/2 activity (10). Surprisingly a Raf mutant that cannot bind MEK or activate ERK1/2 can still affect transcription and RSK activity (38). We therefore examined whether this activated Raf mutant (c-Raf-BXBT481A) could suppress integrin activation in CHO cells. Indeed, we observed suppression of integrin activation (Fig. 1A) that was similar to cells transfected with oncogenic H-Ras (H-RasG12V; Fig. 1B). We therefore investigated the effects of RSK2 activation on integrins. We found that transfection of a dominant active form of RSK2 (RSK2-Y707A) also suppressed integrin activation to a similar level as H-Ras (Fig. 1B). Moreover, H-Ras suppression of integrin activity was abrogated by co-expression of dominant-nega-

RSK2 Suppresses Integrin Activation

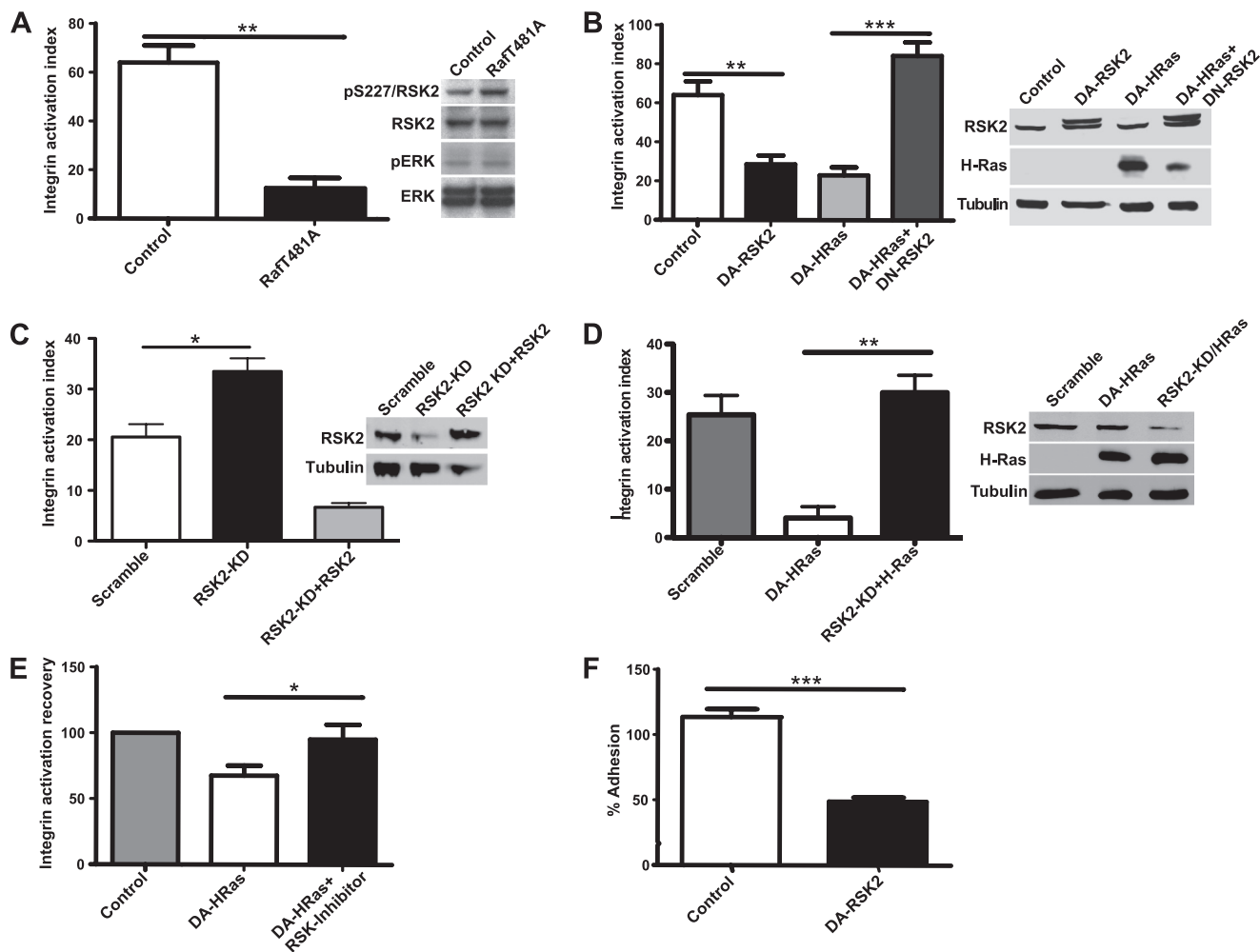


FIGURE 1. RSK2 inhibits integrin activation and impairs cell adhesion. *A* and *B*, CHO1 cells expressing chimeric α IIb β 3 were transiently transfected with control vector (control) and c-RafBXB-T481A mutant (3 μ g) that activates RSK2 independently of ERK (as reported in Ref. 38 and verified by immunoblotting) (*A*) or control vector (control), DA-RSK2 (RSK2-Y707A, 3 μ g), activated DA-H-Ras (H-RasG12V, 3 μ g), or activated DA-H-Ras in combination with DN-RSK2 (H-RasG12V and RSK2-K100A, 3 μ g each) (*B*). *C* and *D*, HeLa cells with stable knockdown of RSK2 were transiently transfected with HA-RSK2 (5 μ g) (*C*) or with activated DA-H-Ras (H-RasG12V, 3 μ g) (*D*). *D*, additionally, HeLa cells stably expressing scrambled shRNA were also transiently transfected with activated DA-H-Ras (H-RasG12V, 3 μ g). Integrin activation was measured by incubating the cells with the ligand-mimetic antibody PAC1 or 3FN-(9–11) ligand and further analysis by three-color flow cytometry. The percentage of activation is shown. The error bars represent S.E. Statistical significance was determined using one-way analysis of variance ($n = 3$; **, $p < 0.01$; ***, $p < 0.001$). *E*, CHO1 cells were transiently transfected with control vector (control) or activated DA-H-Ras (H-RasG12V, 3 μ g) and treated for 24 h with carrier or RSK2 inhibitors, FMK (20 μ M), or SL0101-1 (100 μ M). Integrin activation recovery was normalized versus control cells. The error bars represent S.E. Statistical significance was determined using the Student's *t* test. *F*, CHO1 cells were transiently transfected with control vector or DA-RSK2 (RSK2-Y707A, 3 μ g). 48 h after transfection, the cells were subjected to a cell adhesion assay to fibronectin. Adherent cells were quantified at 1 h using UV-VIS spectrophotometer. The numbers of cells have been normalized to 100% input – a maximal number of cells that could adhere. The error bars represent S.E. Statistical analysis was determined using the Student's *t* test ($n = 6$; ***, $p < 0.0001$). All of the experiments were performed at least three times.

tive RSK2 (Fig. 1*B*) or by RSK2 inhibitors (Fig. 1*E*) in CHO cells. We alternatively investigated whether stable knockdown of RSK2 altered integrin activity in the cervical cancer HeLa cell line. Indeed knockdown of RSK2 caused a significant increase in integrin activation in these cells, and this was rescued by expression of wild-type RSK2 (Fig. 1*C*). Importantly, the suppressive effect of active RSK2 on integrin activation also impaired integrin-mediated cell adhesion to fibronectin, which was inhibited ~3-fold by the dominant active RSK2 (Fig. 1*F*). These findings confirm that RSK2 inactivates integrins and is a principal mediator of Ras signaling to integrins.

RSK2 Inhibits Integrin-mediated Fibronectin Matrix Assembly—Integrin activation and interaction with the cytoskeleton are required for the assembly of a FN matrix on the cell

surface (9). We therefore tested whether activated RSK2 alters FN matrix assembly. We examined the assembly of exogenous labeled FN on the surface of HeLa cells transfected with dominant active RSK2 or control vector. Immunostaining for the presence of fibronectin matrix formation demonstrated that activated RSK2 inhibits FN matrix assembly (Fig. 2, *A* and *B*). To quantitatively measure this effect, we isolated DOC-insoluble fibronectin matrix and determined the amount of FN matrix via immunoblotting. This supported our observation that cells expressing dominant active RSK2 assembled much less matrix compared with their control counterparts (Fig. 2*C*). Finally, in HeLa cells treated with the RSK2 inhibitor, FMK, we found a significant increase in FN matrix assembly over control Me₂SO-treated cells (Fig. 2*D*). Thus, activated RSK2 impairs fibronectin matrix assembly.

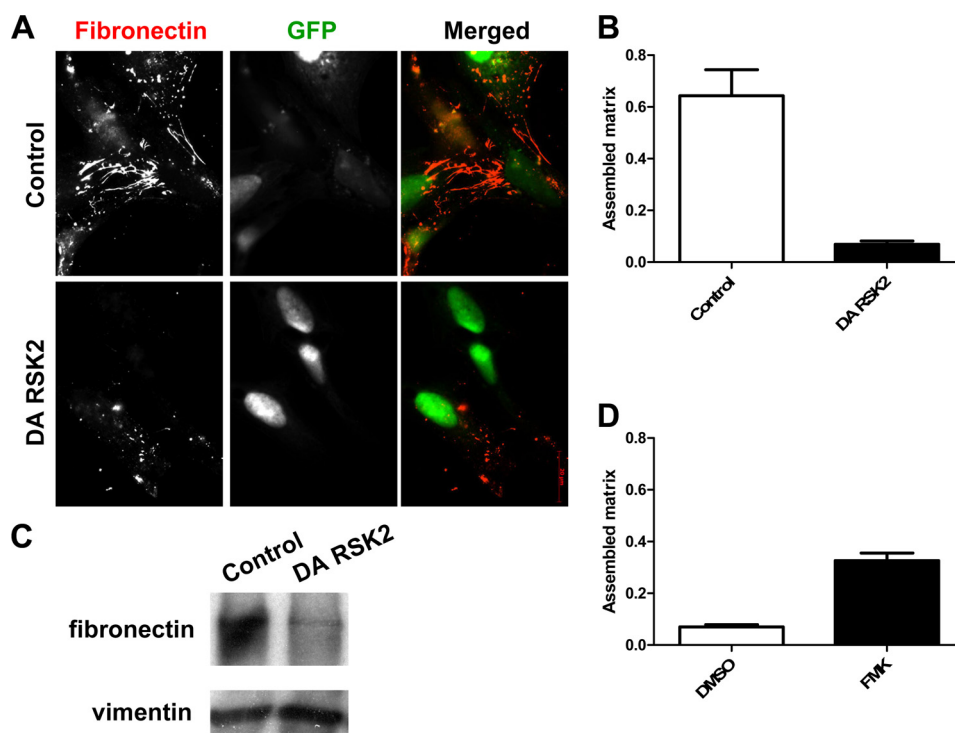


FIGURE 2. RSK2 inhibits fibronectin matrix assembly. HeLa cells were transiently transfected with control vector or DA-RSK2 (RSK2-Y707A, 3 μ g) and with GFP (pEGFP-C1, 1 μ g) as a transfection marker. *A*, cells were fixed and stained with antifibronectin antibody upon 24 h of treatment with human fibronectin and examined by immunofluorescence using a Zeiss Axiovert 200M inverted fluorescent microscope. *B*, matrix assembly was quantified using ImageJ WCIF image analysis software. *C*, an equivalent set of cells was treated with human fibronectin for 36 h, washed, lysed in DOC buffer, and analyzed for fibronectin matrix assembly by immunoblotting. Equal protein loading was verified using an antibody against vimentin. Shown is a representative experiment of at least three repeats. *D*, fibronectin matrix assembly in HeLa cells after treatment with the RSK2 inhibitor FMK (20 μ M) was analyzed and compared with a control treatment with the carrier Me₂SO (DMSO).

RSK2 Enhances Integrin-mediated Cell Migration—Active RSK2 regulates integrin activation and function in both cell adhesion and matrix assembly. Integrin activation can modulate migration (39). We find that overexpression of constitutively active RSK2, in a similar manner as overexpression of active H-Ras, increased the number of cells migrating through the membrane of a Transwell plate \sim 2-fold (Fig. 3A). Similarly, active RSK2 gradually promotes cell migration through the time course of 24 h in an *in vitro* scratch assay (Fig. 3B) and resulted in a nearly 2-fold increase in scratch filling at the 24-h time point (Fig. 3C). Additionally, in the same assay inhibition of endogenous RSK with the FMK inhibitor resulted in significantly suppressed cell motility (Fig. 3D; ***, $p < 0.0001$). The RSK inhibitors did not affect cell viability in these assays (Fig. 3E). Inhibition of RSK with the inhibitor SL0101-1 also blocked the motility of human prostate cancer cells (DU-145). In a two-chamber assay, DU-145 cells migrated significantly less when treated with SL0101-1. In contrast, migration of human mesothelioma cells (MILL) remained unaffected after treatment with the RSK inhibitor (Fig. 3F). The viability of the cells was not significantly altered in these assays (Fig. 3G). Thus, RSK can modulate migration in some but not all cancer cells.

RSK2 Disrupts Actin Stress Fibers and Focal Adhesions and Co-localizes with Talin—Integrin function in cell adhesion, migration, and matrix assembly requires interaction with the actin cytoskeleton (40). Integrin cytoplasmic tail domains associate with cytoskeletal proteins including talin, filamin A, vinculin, and α -actinin (40). The cytoskeletal protein associated

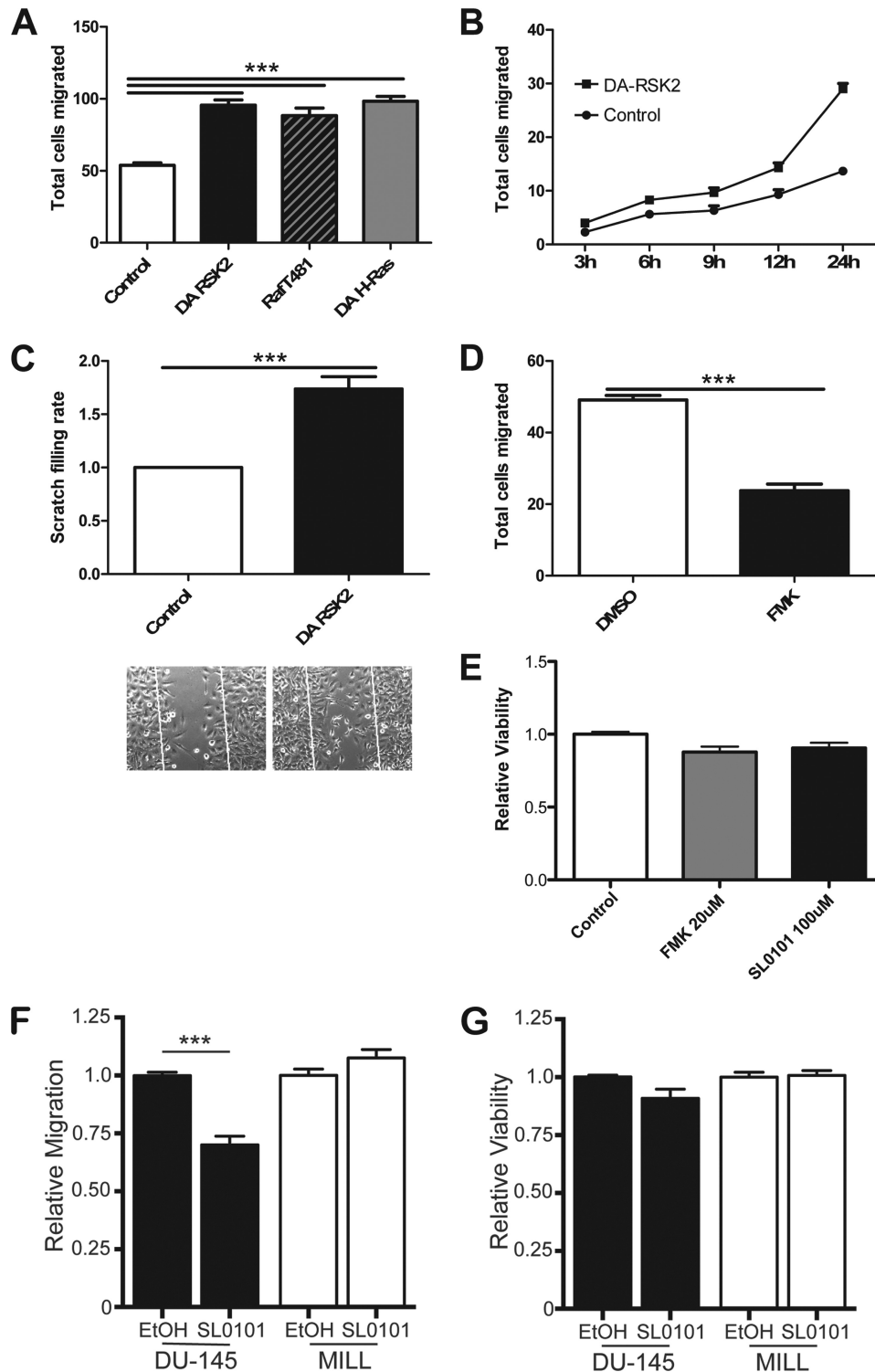
with the integrin may, in part, determine the function of the integrin. The Ras/MAPK pathway plays an important role in cytoskeletal remodeling. Ras-transformed cells lose actin stress fibers and exhibit a round, spindle-like morphology (41). We therefore investigated whether activated RSK2 affects cytoskeletal structure in HeLa cells. We found that expression of active RSK2 correlated with severe disruption of actin fibers (Fig. 4A). We noted that 83% of cells transfected with active RSK2 lacked actin fibers, compared with only 19% of control cells. Importantly, we saw that RSK2 altered the localization of talin. Talin binds integrins at membrane-localized sites called focal adhesions, and this binding is required for integrin activation (24, 34). We observed that active RSK2 altered talin localization in focal adhesions (Fig. 4B). Although the talin was observed in punctate structures at the plasma membrane, it no longer showed the characteristic elongated localization along the tips of the actin fibers as seen in control cells. Instead, talin was observed in larger and rounded plasma membrane localized regions. Thus, the functional effects of RSK2 on integrins may result from changes in the association of the integrins or talin with the cytoskeleton.

We next determined whether endogenous RSK2 activity similarly affected actin and talin distribution in migrating cells. We plated cells on coverslips and, after they reached confluence, made a scratch. We examined talin and actin at the leading edge in cells stimulated with EGF in the presence and absence of the RSK inhibitor SL0101-1. We found that EGF stimulation leads to peripheral ruffle formation and redistribu-

RSK2 Suppresses Integrin Activation

tion of talin at the leading edge of cells entering the scratch (Fig. 5, compare *A* and *C*). However, when the cells are treated with SL0101-1 in addition to EGF, talin remains predominantly at the focal adhesions, and actin filaments become stabilized at the leading edge (Fig. 5, *B* and *D*). Indeed, the actin stress fibers lack organization in these cells. Thus, endogenous RSK activity is required for redistribution of actin and talin associated with migration.

Talin binds directly to integrins (42), and this binding is required for integrin activation (24, 26). This interaction takes place at focal adhesions and provides a link between integrins and the actin cytoskeleton (40). We found that endogenous RSK2 localizes at the tips of actin fibers in HeLa cells and that active RSK2 co-localized with talin, primarily at the cell membrane (Fig. 6). Therefore, RSK2 is in a position to affect integrin activation and interaction with the actin cytoskeleton.



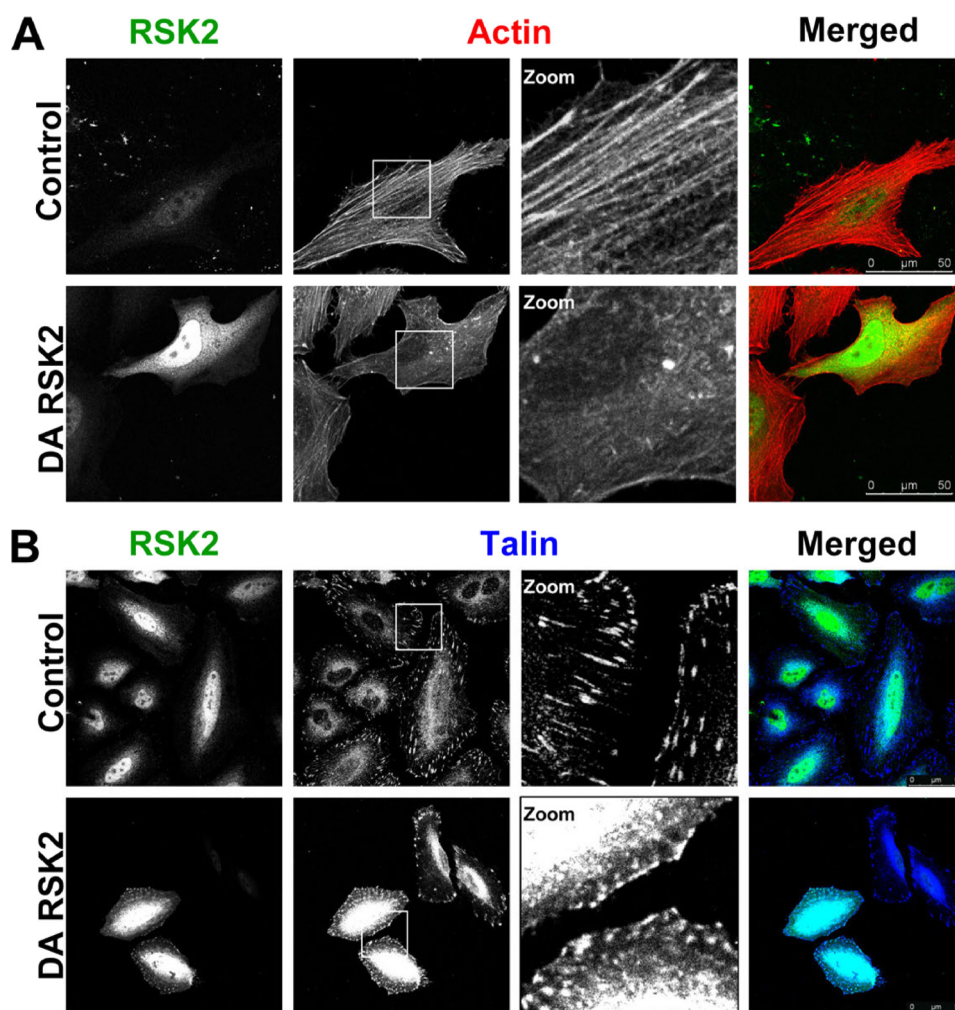


FIGURE 4. RSK2 disrupts actin cytoskeleton and focal adhesions. *A*, HeLa cells were transiently transfected with DA-RSK2 (Y707A) or control vector. After 48 h, the cells were fixed and stained for RSK2 (green) and actin (red). *B*, HeLa cells were transiently transfected with talin (3 μ g) and DA-RSK2 (RSK2-Y707A, 3 μ g) or control vector (3 μ g). 48 h after transfection, the cells were fixed and stained for RSK2 (green) and talin (blue). Immunostaining was visualized using a Leica TCS SP5 confocal microscope. Shown is a representative experiment of at least three repeats. The scale bars shown represent 50 μ m.

RSK2 Associates with Integrin Cytoplasmic Tails—The cytoplasmic tail domains of integrins serve as anchors to the cytoskeleton and, by mediating signals from both the outside and inside of the cells, can play an important role in integrin function such as cellular adhesion or migration (40). RSK2 co-localizes with talin. We therefore investigated whether RSK2 associated with integrin cytoplasmic tails. We used His-tagged integrin tails immobilized on Sepharose beads to pull down

proteins from CHOK1 cells transfected with dominant active RSK2 (Fig. 7A). Integrin tail expression and RSK2 transfection levels are shown in Fig. 7 (B and C), respectively. Note that there is significant endogenous RSK2 (Fig. 7C). We found that RSK2 associated with the integrin β 1 and β 7 tail proteins, whereas we saw no association of RSK2 with control α IIb tail proteins (Fig. 7A). As previously reported (34), we found that both filamin and talin also associated with the tails, and active RSK2 expres-

FIGURE 3. RSK2 enhances cell migration on fibronectin. *A*, HeLa cells were transfected with 2 μ g of the indicated plasmids in combination with a vector expressing β -galactosidase. The cells were plated in the upper chamber of a Transwell plate. The lower side of the membrane was coated with fibronectin (10 μ g/ml). After 6 h, the total number of transfected cells that had migrated through to the bottom of the membrane was counted in random fields using a blinded analysis. The error bars represent S.E. Statistical significance was determined using the one-way analysis of variance ($n = 4$; ***, $p < 0.0001$). *B* and *C*, HeLa cells were transiently transfected with activated RSK2 or control vector. 24 h later, the cell monolayer was scratched with a micropipette tip. The scratch filling process was documented using Zeiss Axiovert 200M inverted microscope. *B*, the total number of cells that migrated into the scratch area was counted at various time points. *C*, relative scratch filling rate was calculated at 24 h. The inset shows a representative image of scratch after 24 h of recovery time. The error bars represent S.E. Statistical significance was determined using Student's *t* test ($n = 4$; ***, $p < 0.001$). *D*, HeLa cells were treated with either the RSK2 inhibitor FMK (20 μ M) or Me₂SO (DMSO) as a carrier control, and the cell monolayer was scratched with a micropipette tip. The scratch filling process was determined by phase imaging using a Zeiss Axiovert 200M inverted microscope. The total number of cells that migrated into the scratch area was counted at 24 h. The error bars represent S.E. Statistical significance was determined using the Student's *t* test ($n = 9$; ***, $p < 0.0001$). *E*, HeLa cell viability in these assays upon exposure to FMK (20 μ M) or SL0101-1 (100 μ M) was determined by XTT assay. Shown is the relative viability corrected to a treatment with the carrier control ($n = 3$). *F*, migration of cancer cell lines (DU-145 and MILL) upon exposure to SL0101-1 (100 μ M) was determined using a two-chamber migration assay with fibronectin-coated inserts and EGF as chemoattractant. After 20 h, the cells that migrated to the bottom side of the insert were stained with Calcein-AM and quantified measuring the fluorescence emission at 520 nm. *G*, cell viability upon exposure to SL0101-1 (100 μ M) was determined by XTT assay. *F* and *G*, bar graphs show the relative amount of migration or relative viability compared with cells treated with the carrier EtOH. The error bars represent S.E. Statistical significance was determined using the Student's *t* test ($n = 3$; ***, $p < 0.0001$).

RSK2 Suppresses Integrin Activation

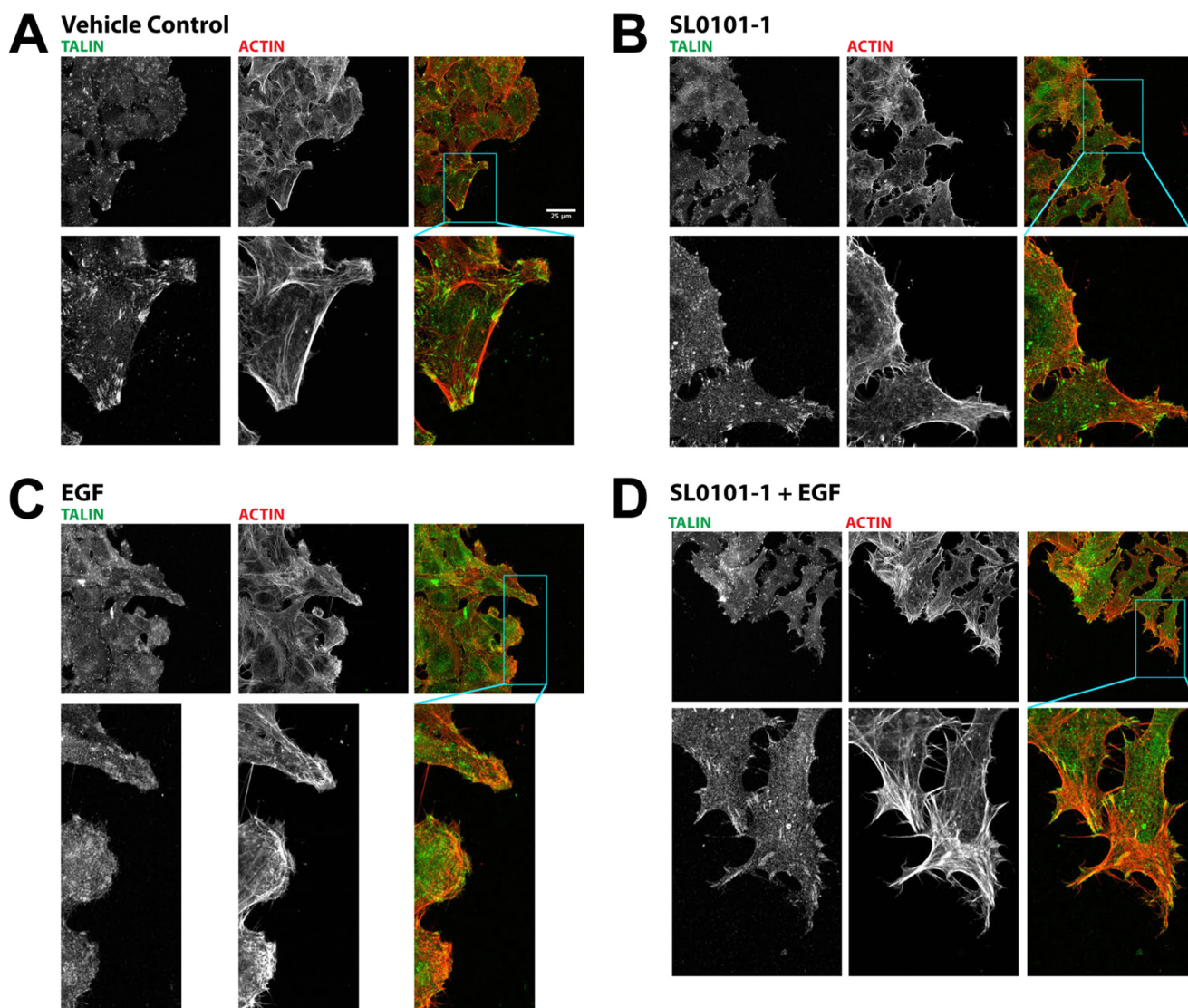


FIGURE 5. RSK2 activity is required for actin and talin rearrangements that promote migration. HeLa cells were seeded on fibronectin-coated glass coverslips and allowed to grow to confluence. Growth medium was then replaced with medium containing 0.5% serum and incubated overnight. The coverslips were scratched with a micropipette tip and then treated with vehicle (A), SL0101-1 (100 μM) (B and D), or EGF (100 ng/ml) (C and D) and allowed to incubate an additional 2 h followed by fixation. The coverslips were then stained with phalloidin and antibody against talin to visualize actin and focal adhesions by confocal microscopy. Treatment with EGF leads to peripheral ruffle formation and redistribution of talin. However, when the cells are treated with SL0101-1 in addition to EGF, talin remains predominantly at the focal adhesions, and actin filaments become stabilized at the leading edge. The scale bars shown represent 25 μm .

sion did not affect this interaction (Fig. 7A). We next examined whether RSK2 bound to the NPXY mutant (Y788A) of the $\beta 1$ tail that does not bind talin. We found that RSK2 also binds this mutant, whereas talin did not, indicating that RSK2 binds integrin tail complexes independently of talin (Fig. 7D). Endogenous RSK2 co-localized with talin by immunofluorescence and over-expressed activated DA-RSK2 binds integrins tail complexes. We next determined whether endogenous RSK2 can bind the integrin tail complex and whether RSK2 activity affects this binding. To address this question, we examined integrin tail binding of endogenous RSK2 from CHO cells where RSK2 is activated by EGF or its activation is blocked by the MEK inhibitor U0126. We found that endogenous RSK2 binding to the tails is unaffected by EGF stimulation, and both the phosphorylated RSK2 and nonphosphorylated RSK2 can bind the purified tails (Fig. 7E).

Talin proteolysis by the calcium-dependent protease calpain alters cell adhesion and migration (43, 44). Calpain cleavage of intact talin was reported to release the talin head domain and increase talin binding to integrin β tails (45). We investigated whether the enforced expression of dominant active RSK2 affects talin cleavage. We found no difference in talin cleavage in the cells expressing constitutively active RSK2 compared with control cells. We also report no difference in cleavage of either filamin A phosphorylated at an RSK2 substrate site (Ser-2152) or total filamin A (Fig. 7F).

RSK2 Phosphorylates Filamin A and Promotes Its Binding to Integrin Tails—To further investigate how RSK2 modulates integrin activation, we examined whether purified RSK2 could phosphorylate proteins that bind the integrin tails. We found that a band of 260–280 kDa was phosphorylated (Fig. 8A). This corresponds to the size of filamin (280 kDa) or talin (260 kDa).

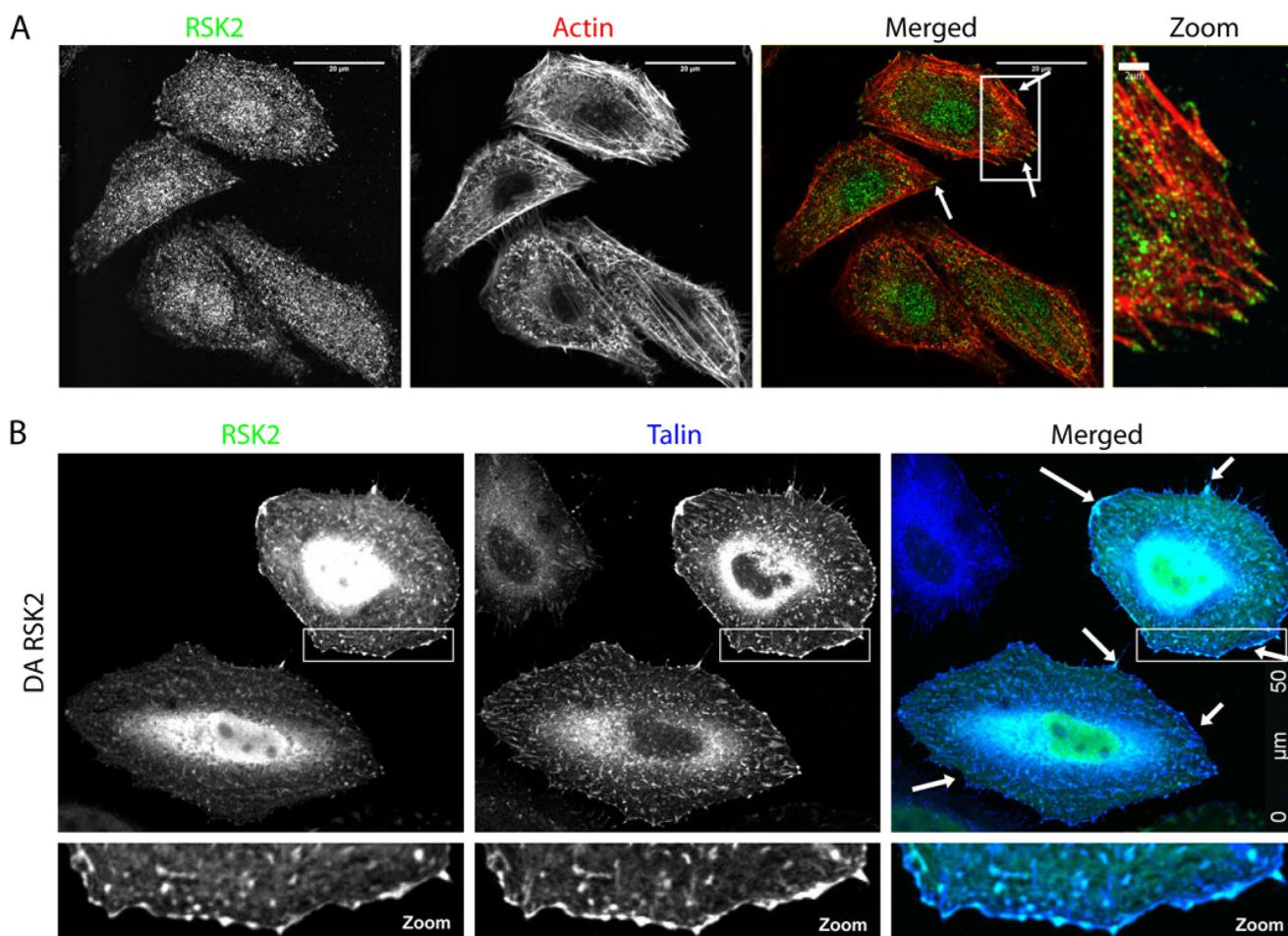


FIGURE 6. **RSK2 co-localizes with the integrin activator protein talin.** *A*, HeLa cells were plated on fibronectin-coated (10 $\mu\text{g}/\text{ml}$) coverslips. The cells were serum-starved (0.5% FBS) for 18 h and subsequently fixed and immunostained for RSK2 (green) and for actin using rhodamine phalloidin (red). *B*, HeLa cells were transiently transfected with DA-RSK2 (RSK2-Y707A, 3 μg) and talin (3 μg). At 48 h post-transfection, the cells were fixed and stained for RSK2 (green) and talin (blue). Co-localization was examined using a Leica TCS SP5 confocal microscope. The scale bars shown represent 20 μm (or 2 μm in zoom) in *A* and 50 μm in *B*.

We therefore determined whether RSK2 could directly phosphorylate talin and RSK2. Purified active RSK2 did not phosphorylate talin but did phosphorylate filamin A as previously reported (46, 47) (Fig. 8B). We further showed that the site phosphorylated was identical to that previously reported (Ser-2152; Fig. 8C). Phosphorylation at this site had been previously reported to affect cell migration, but no mechanism was identified. We tested the hypothesis that the phosphorylation might alter filamin binding to the integrin tails. Indeed phosphorylation of filamin by active RSK2 promoted binding of filamin to the integrin tails (Fig. 8D). If RSK2 activity is required to promote filamin binding to the tails, then inhibition of RSK2 should impair filamin binding. We therefore incubated CHOK1 cells in the RSK2 inhibitor SL0101 and then ran lysates from these cells over our tail proteins. We found that filamin from cells where RSK2 was inhibited failed to bind the tails, whereas control carrier-treated cells contained filamin that could bind (Fig. 8E). Therefore, RSK2 activity is required for filamin binding to integrin tails.

RSK2 Is Activated upon Integrin Ligation to Fibronectin—Integrins play a principal role in regulation of cell migration. They not only act as adhesion receptors but also initiate multiple signaling cascades including Ras activated pathways (5). We

therefore examined whether integrin ligation altered activation of endogenous RSK2 in CHOK1 cells. Indeed, we found that RSK2 was activated in response to integrin engagement of fibronectin (Fig. 9A). Interestingly, both autophosphorylation at Ser-386 and tyrosine phosphorylation, thought to be mediated by Src (48), at Tyr-529 increase after replating cells on fibronectin. This suggests that integrins may activate a feedback loop upon binding to extracellular matrix that leads to inactivation of other integrins perhaps contributing to a cycling of activation during migration. RSK2 therefore can dynamically regulate integrin activation.

DISCUSSION

Modulation of integrin affinity for ligand is important in a broad array of cellular functions including adhesion, migration, signal transduction, and the assembly of extracellular matrix. Changes in integrin activation are also linked to diverse diseases including cancer metastasis (1). Therefore, understanding the regulatory mechanisms involved is essential in development of novel cancer therapeutics. Here we report that RSK2 regulates integrin activation and mediates the suppression of integrin activity by the oncogene H-Ras. The functional consequence of RSK2 regulation of integrins is inhibition of fibronectin matrix

RSK2 Suppresses Integrin Activation

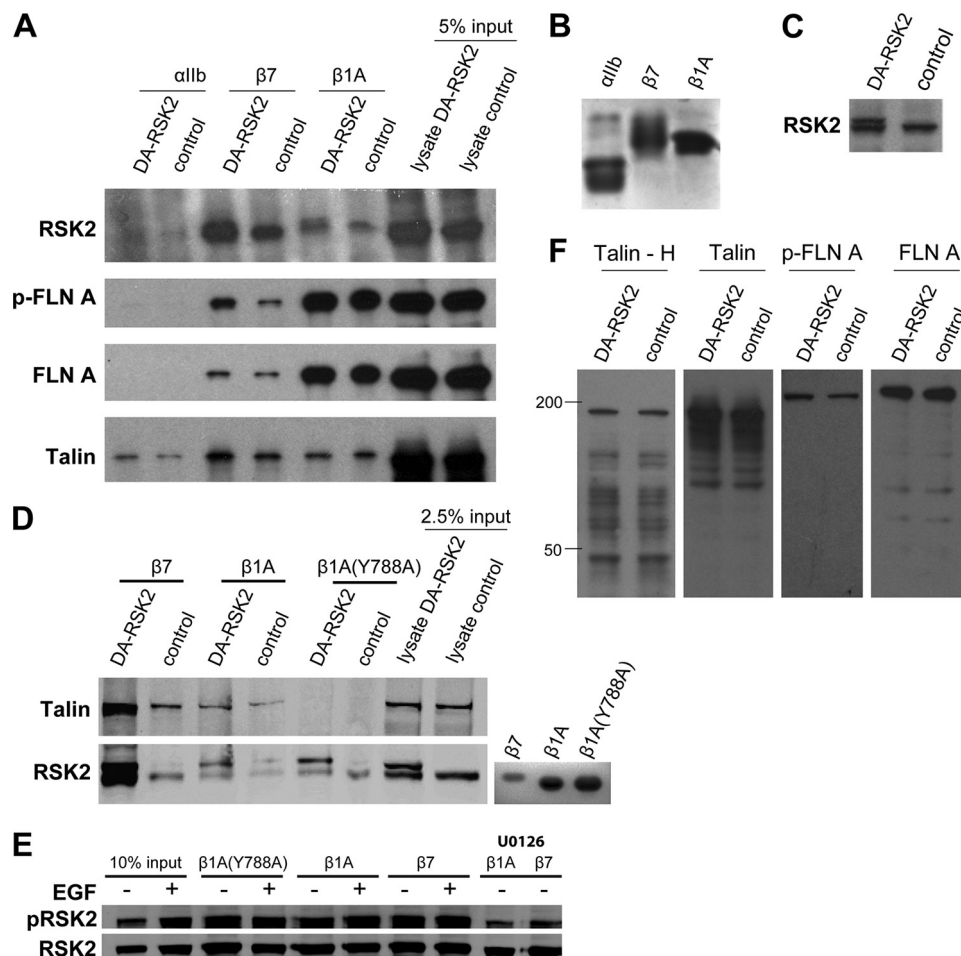


FIGURE 7. RSK2 associates with integrin cytoplasmic tail complexes, phosphorylates filamin, and promotes filamin binding to integrin tails. CHOK1 cells were transfected with DA-RSK2 (RSK2-Y707A, 3 μ g) or control vector (3 μ g). 48 h after transfection, the cells were lysed and incubated with bead-bound purified integrin cytoplasmic domains. **A**, precipitated proteins were detected by immunoblotting as indicated. **B**, bead-bound purified integrin cytoplasmic tail expression was verified by Coomassie staining. **C**, RSK2 transfection efficiency was verified by immunoblotting of whole cell lysates. **D**, CHOK1 cells were transfected as in **A**. Bound RSK2 and talin were detected by immunoblotting as indicated. **E**, serum-starved CHOK1 cells were treated with EGF (50 μ M), MEK inhibitor (U0126, 10 μ M), or carrier alone (Me₂SO). The cells were lysed and incubated with bead-bound purified integrin cytoplasmic domains. Bound protein was analyzed by immunoblotting to determine the amount of pS386-RSK2 or total RSK2 bound. **F**, degradation of talin was determined by immunoblotting using an antibody specific to the talin head domain (*Talin - H*) or an antibody that recognizes an epitope in the talin rod domain. Degradation of filamin A phosphorylated at Ser-2156 and total filamin A were verified by immunoblotting of whole cell lysates. All of the data are representative of experiments performed at least three times.

assembly, inhibition of cell adhesion, and enhancement of cell migration. Our data indicate that RSK2 in both its active and inactive state can localize to the complex of proteins binding the integrin β tails. RSK2 can bind the NPXY β 1 integrin mutant and thereby bind the tail complex in the absence of talin. Therefore, upon activation, RSK2 can immediately phosphorylate filamin A and thus promote its binding to integrin tails. This in turn alters interaction of the tail-binding complex with the actin cytoskeleton, thereby disturbing the formation of actin stress fibers (Fig. 9B). It is noteworthy that although we saw a clear increase in filamin binding to the tails, we did not see a significant change in talin binding in either our immunofluorescence or tail pulldown assays. It may be that filamin A binding to the tails displaces talin head domain association with the integrins as reported (49) but that talin remains associated with the integrins through interactions at its other integrin binding sequences in the rod domain. This remains to be determined. Finally, integrin ligation activates RSK2 and may be involved in dynamic regulation of integrin activity during cell adhesion and

migration. We propose that RSK2 function in migration and metastasis is mediated in part by changes in integrin affinity for extracellular matrix proteins.

The H-Ras activated MAPK pathway suppresses integrin activation by a transcription-independent mechanism (7). This suppression does not require bulk activation of ERK1/2 MAP kinase, nor was it reversed by an inhibition of ERK activation (10). This effect is suppressed by a protein called PEA-15 (30). We previously reported that PEA-15 binds to and inhibits RSK2 function when overexpressed (50). Interestingly PEA-15 also blocks cell migration and metastasis (51, 52). It is therefore possible that PEA-15 will affect integrins because of its inhibition of RSK2 function. We also found that a Raf construct that does not bind MEK or activate ERK could nevertheless inactivate integrins. This is in agreement with previous reports that ERK activity is not required for Ras or Raf suppression of integrin activation (10). This further establishes that Raf may use ERK-independent signaling routes to inhibit integrins.

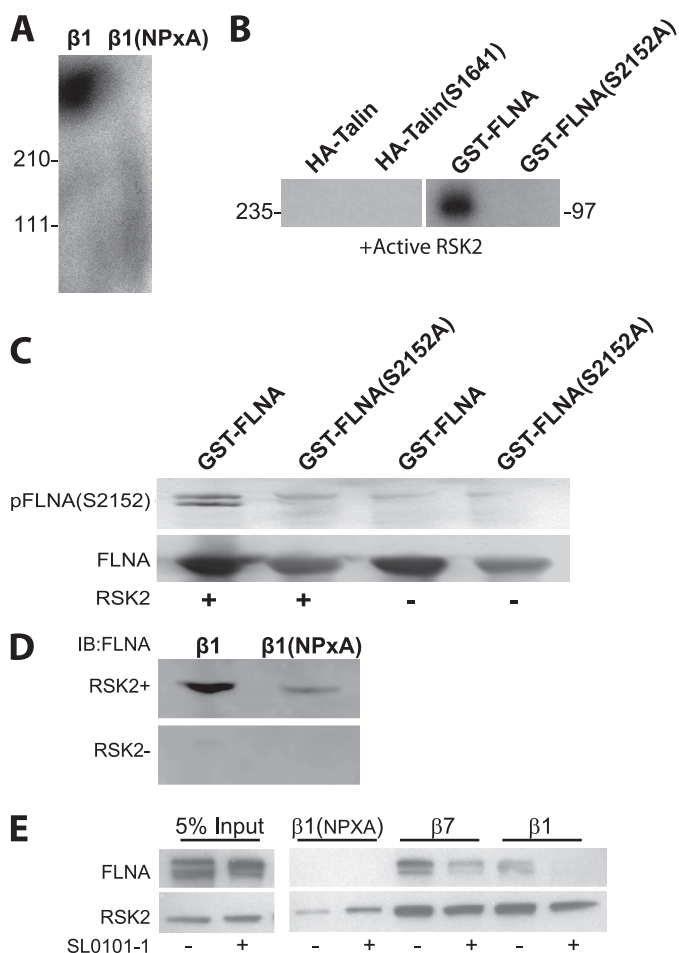


FIGURE 8. RSK2 phosphorylates filamin A and promotes its binding to integrin tails. *A*, integrin tail complexes were prepared by incubating serum-starved CHOK1 cell lysates with integrin cytoplasmic domains bound to beads. They were then washed and incubated with purified active RSK2 in a kinase buffer with [γ - 32 P]ATP. The autoradiograph is shown. *B*, RSK2 phosphorylation of talin and filamin A was determined similarly by a kinase assay using [γ - 32 P]ATP. HA-tagged talin was immunoprecipitated from lysates prepared from serum-starved CHOK1 cells that were transiently transfected with HA-talin (3 μ g) or HA-talin (S1641A) (3 μ g). Alternatively, recombinant GST-filamin A (10 μ g) and phospho-mutant GST-filamin A (S2152A) (10 μ g) were also examined. *C*, RSK2 phosphorylation of recombinant GST-filamin A (10 μ g) and phospho-mutant GST-filamin A (S2152A) (10 μ g) was further tested by immunoblotting with an antibody specific for Ser-2152 phosphorylated filamin. The bottom panel represents a Coomassie stain of purified glutathione-agarose-bound filamin A proteins. *D*, lysates from serum-starved CHOK1 cells were incubated with purified RSK2 or control in kinase buffer. Filamin binding to the tails was determined by immunoblot (*IB*). *E*, CHOK1 cells were incubated with RSK2 inhibitor (100 μ M) or control carrier ethanol for 30 min. Lysates from these cells were then run over integrin cytoplasmic tail proteins to determine filamin A binding to integrin β 7, β 1, and β 1 (NPXA) mutants. Input of 5% served as a control for the presence of filamin A and RSK2.

The suppressive effect that RSK2 has on integrin activation also impairs integrin function. Dominant active RSK2 blocks cell adhesion and greatly impairs integrin-mediated fibronectin matrix assembly, thereby promoting a highly motile, invasive metastatic phenotype in transfected cells. Furthermore, the constitutively active RSK2 significantly increases cell migration, whereas inhibition of endogenous RSK2 with FMK inhibitor results in suppressed cell motility. These data are in agreement with recent reports that RSK2 acts as a principal regulator of the invasive phenotype of epithelial cells, as well as a key promoter of human head and neck cancer metastasis (13, 15).

Raf suppression of integrin activity is independent of transcription, and it is thus likely that RSK2 effects on integrin activity are similarly transcription independent. Moreover, we found that a Raf mutant that activates RSK2 independently of MEK and ERK nevertheless suppresses integrin activation and enhances migration in a manner similar to that of RSK2. We therefore suggest that RSK2 mediates Raf-driven migration in a manner independent of transcription.

In addition to enhanced migration, we also demonstrated that expression of active RSK2 disorganizes the actin cytoskeleton and disrupts focal adhesions. The effect is similar to that of active H-Ras, which also disrupts focal adhesions and the actin cytoskeleton (41). Both extracellular matrix assembly and focal adhesion formation require integrin interaction with the cell cytoskeleton (9, 22) and are increased by integrin interactions with talin (34, 53). Thus, RSK2 appears to alter integrin activation by interfering with the interaction of talin, filamin, and potentially other cytoskeletal proteins with the integrin and the actin cytoskeleton.

Additionally we find that RSK2 co-localizes with the integrin activator talin and is present in the complex at integrin cytoplasmic tails. RSK2 is therefore in a location where it can directly modulate regulation of integrin activation. Importantly, the integrin tails themselves do not contain consensus sequences for RSK2 phosphorylation, and RSK2 does not phosphorylate them directly. Talin and filamin A are actin-binding proteins that form the cytoplasmic face of focal adhesions (54); however, their role in the actin cytoskeleton complex differs significantly. Filamin A associates with microfilament bundles, and the stress fiber ends at focal contacts and stabilizes actin filament aggregates (54). Talin nucleates, caps, and cross-links actin filaments and serves as the structural component of cell-matrix adhesions but not cell-cell contacts (54). Our observation of the disruptive effect RSK2 has on cytoskeleton arrangement and its suppressive effect on integrin affinity suggest that RSK2 affects talin function in focal adhesions. For example, it may affect talin translocation to newly formed focal adhesions. This subcellular translocation was reported previously to accompany increases in talin phosphorylation (54–56). We find that RSK2 phosphorylates filamin at serine 2152 as previously reported (46, 47) but does not phosphorylate talin. Phosphorylation of filamin leads to increased filamin binding to the integrin tails, and this corresponds to the inactivation of the integrin, as well as changes in the actin cytoskeleton. We did not find differences in talin binding to the integrin tails in response to RSK2 activity, and indeed, it appears that talin remains associated with the integrin tails in the presence of active RSK2. We hypothesize that increased filamin binding to the integrins displaces the talin head domain as previously reported (49) but that talin persists in the complex because of other interactions. Thus, RSK2 may modulate integrin activation in part through direct phosphorylation of filamin.

We conclude that RSK2 suppresses integrin activation downstream of the oncogene H-Ras. Both RSK2 and changes in integrin activation are linked to cancer metastasis. Therefore, because of its involvement in the regulation of integrin activation and its role in promoting a motile, metastatic cell phenotype, RSK2 is a potentially interesting target for antimetastasis therapies.

RSK2 Suppresses Integrin Activation

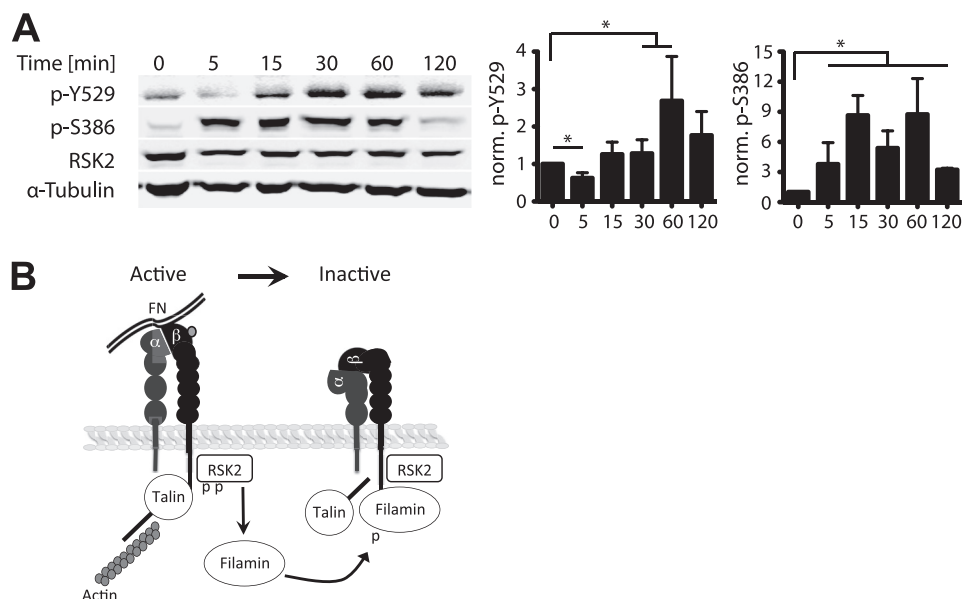


FIGURE 9. RSK2 phosphorylation increases upon integrin binding to matrix. *A*, CHOK1 cells were grown to confluence, lifted from the dish with nonenzymatic cell dissociation buffer, and allowed to adhere to fibronectin-coated cell culture plates for 0 min, 5 min, 15 min, and 30 min, 1 h, or 2 h. The cells were then lysed, and RSK2 phosphorylation was determined by immunoblotting. Actin was used as a loading control. *B*, diagram showing that integrin or growth factor receptor signaling activates RSK2. Active RSK2 then phosphorylates filamin at serine 2152 promoting filamin binding to the integrin. This alters the actin, talin, and integrin complex leading to the release of actin, reorganization of talin localization, and subsequent integrin inactivation. This cycle may facilitate cell migration and interfere with FN matrix assembly.

REFERENCES

- Felding-Habermann, B., O'Toole, T. E., Smith, J. W., Fransvea, E., Ruggeri, Z. M., Ginsberg, M. H., Hughes, P. E., Pampori, N., Shattil, S. J., Saven, A., and Mueller, B. M. (2001) Integrin activation controls metastasis in human breast cancer. *Proc. Natl. Acad. Sci. U.S.A.* **98**, 1853–1858
- Guo, W., and Giancotti, F. G. (2004) Integrin signalling during tumour progression. *Nat. Rev. Mol. Cell Biol.* **5**, 816–826
- Mehlen, P., and Puisieux, A. (2006) Metastasis. A question of life or death. *Nat Rev Cancer* **6**, 449–458
- Schwartz, M. A. (1997) Integrins, oncogenes, and anchorage independence. *J. Cell Biol.* **139**, 575–578
- Hynes, R. O. (2002) Integrins. Bidirectional, allosteric signaling machines. *Cell* **110**, 673–687
- Kinbara, K., Goldfinger, L. E., Hansen, M., Chou, F. L., and Ginsberg, M. H. (2003) Ras GTPases. Integrins' friends or foes? *Nat. Rev. Mol. Cell Biol.* **4**, 767–776
- Hughes, P. E., Renshaw, M. W., Pfaff, M., Forsyth, J., Keivens, V. M., Schwartz, M. A., and Ginsberg, M. H. (1997) Suppression of integrin activation. A novel function of a Ras/Raf-initiated MAP kinase pathway. *Cell* **88**, 521–530
- Brenner, K. A., Corbett, S. A., and Schwarzbauer, J. E. (2000) Regulation of fibronectin matrix assembly by activated Ras in transformed cells. *Oncogene* **19**, 3156–3163
- Wu, C., Keivens, V. M., O'Toole, T. E., McDonald, J. A., and Ginsberg, M. H. (1995) Integrin activation and cytoskeletal interaction are essential for the assembly of a fibronectin matrix. *Cell* **83**, 715–724
- Hughes, P. E., Oertli, B., Hansen, M., Chou, F. L., Willumsen, B. M., and Ginsberg, M. H. (2002) Suppression of integrin activation by activated Ras or Raf does not correlate with bulk activation of ERK MAP kinase. *Mol. Biol. Cell* **13**, 2256–2265
- Anjum, R., and Blenis, J. (2008) The RSK family of kinases. Emerging roles in cellular signalling. *Nat. Rev. Mol. Cell Biol.* **9**, 747–758
- Carriere, A., Ray, H., Blenis, J., and Roux, P. P. (2008) The RSK factors of activating the Ras/MAPK signaling cascade. *Front. Biosci.* **13**, 4258–4275
- Doehn, U., Hauge, C., Frank, S. R., Jensen, C. J., Duda, K., Nielsen, J. V., Cohen, M. S., Johansen, J. V., Winther, B. R., Lund, L. R., Winther, O., Taunton, J., Hansen, S. H., and Frödin, M. (2009) RSK is a principal effector of the RAS-ERK pathway for eliciting a coordinate promotile/invasive gene program and phenotype in epithelial cells. *Mol Cell* **35**, 511–522
- Smith, J. A., Poteet-Smith, C. E., Xu, Y., Errington, T. M., Hecht, S. M., and Lannigan, D. A. (2005) Identification of the first specific inhibitor of p90 ribosomal S6 kinase (RSK) reveals an unexpected role for RSK in cancer cell proliferation. *Cancer Res.* **65**, 1027–1034
- Kang, S., Elf, S., Lythgoe, K., Hitosugi, T., Taunton, J., Zhou, W., Xiong, L., Wang, D., Muller, S., Fan, S., Sun, S. Y., Marcus, A. I., Gu, T. L., Polakiewicz, R. D., Chen, Z. G., Khuri, F. R., Shin, D. M., and Chen, J. (2010) p90 ribosomal S6 kinase 2 promotes invasion and metastasis of human head and neck squamous cell carcinoma cells. *J. Clin. Invest.* **120**, 1165–1177
- Lara, R., Mauri, F. A., Taylor, H., Derua, R., Shia, A., Gray, C., Nicols, A., Shiner, R. J., Schofield, E., Bates, P. A., Waelkens, E., Dallman, M., Lamb, J., Zicha, D., Downward, J., Seckl, M. J., and Pardo, O. E. (2011) An siRNA screen identifies RSK1 as a key modulator of lung cancer metastasis. *Oncogene* **30**, 3513–3521
- Kang, S., Dong, S., Gu, T. L., Guo, A., Cohen, M. S., Lonial, S., Khoury, H. J., Fabbro, D., Gilliland, D. G., Bergsagel, P. L., Taunton, J., Polakiewicz, R. D., and Chen, J. (2007) FGFR3 activates RSK2 to mediate hematopoietic transformation through tyrosine phosphorylation of RSK2 and activation of the MEK/ERK pathway. *Cancer Cell* **12**, 201–214
- Clark, D. E., Errington, T. M., Smith, J. A., Frierson, H. F., Jr., Weber, M. J., and Lannigan, D. A. (2005) The serine/threonine protein kinase, p90 ribosomal S6 kinase, is an important regulator of prostate cancer cell proliferation. *Cancer Res.* **65**, 3108–3116
- Bignone, P. A., Lee, K. Y., Liu, Y., Emilion, G., Finch, J., Soosay, A. E., Charnock, F. M., Beck, S., Dunham, I., Mungall, A. J., and Ganesan, T. S. (2007) RPS6KA2, a putative tumour suppressor gene at 6q27 in sporadic epithelial ovarian cancer. *Oncogene* **26**, 683–700
- Trivier, E., De Cesare, D., Jacquot, S., Pannetier, S., Zackai, E., Young, I., Mandel, J. L., Sassone-Corsi, P., and Hanauer, A. (1996) Mutations in the kinase Rsk-2 associated with Coffin-Lowry syndrome. *Nature* **384**, 567–570
- Ohta, Y., Suzuki, N., Nakamura, S., Hartwig, J. H., and Stossel, T. P. (1999) The small GTPase RalA targets filamin to induce filopodia. *Proc. Natl. Acad. Sci. U.S.A.* **96**, 2122–2128
- Calderwood, D. A., Huttenlocher, A., Kiosses, W. B., Rose, D. M., Woodside, D. G., Schwartz, M. A., and Ginsberg, M. H. (2001) Increased filamin binding to β -integrin cytoplasmic domains inhibits cell migration. *Nat. Cell Biol.* **3**, 1060–1068
- Calderwood, D. A. (2004) Talin controls integrin activation. *Biochem. Soc.*

- Trans.* **32**, 434–437
24. Calderwood, D. A., Zent, R., Grant, R., Rees, D. J., Hynes, R. O., and Ginsberg, M. H. (1999) The talin head domain binds to integrin β subunit cytoplasmic tails and regulates integrin activation. *J. Biol. Chem.* **274**, 28071–28074
 25. Calderwood, D. A., Yan, B., de Pereda, J. M., Alvarez, B. G., Fujioka, Y., Liddington, R. C., and Ginsberg, M. H. (2002) The phosphotyrosine binding-like domain of talin activates integrins. *J. Biol. Chem.* **277**, 21749–21758
 26. Tadokoro, S., Shattil, S. J., Eto, K., Tai, V., Liddington, R. C., de Pereda, J. M., Ginsberg, M. H., and Calderwood, D. A. (2003) Talin binding to integrin β tails. A final common step in integrin activation. *Science* **302**, 103–106
 27. Moser, M., Legate, K. R., Zent, R., and Fassler, R. (2009) The tail of integrins, talin, and kindlins. *Science* **324**, 895–899
 28. Ye, F., Hu, G., Taylor, D., Ratnikov, B., Bobkov, A. A., McLean, M. A., Sligar, S. G., Taylor, K. A., and Ginsberg, M. H. (2010) Recreation of the terminal events in physiological integrin activation. *J. Cell Biol.* **188**, 157–173
 29. Goksoy, E., Ma, Y. Q., Wang, X., Kong, X., Perera, D., Plow, E. F., and Qin, J. (2008) Structural basis for the autoinhibition of talin in regulating integrin activation. *Mol. Cell* **31**, 124–133
 30. Ramos, J. W., Kojima, T. K., Hughes, P. E., Fenczik, C. A., and Ginsberg, M. H. (1998) The death effector domain of PEA-15 is involved in its regulation of integrin activation. *J. Biol. Chem.* **273**, 33897–33900
 31. Chou, F. L., Hill, J. M., Hsieh, J. C., Pouyssegur, J., Brunet, A., Glading, A., Uberall, F., Ramos, J. W., Werner, M. H., and Ginsberg, M. H. (2003) PEA-15 binding to ERK1/2 MAPKs is required for its modulation of integrin activation. *J. Biol. Chem.* **278**, 52587–52597
 32. Berrier, A. L., and Yamada, K. M. (2007) Cell-matrix adhesion. *J. Cell. Physiol.* **213**, 565–573
 33. Zhang, Z., Vuori, K., Wang, H., Reed, J. C., and Ruoslahti, E. (1996) Integrin activation by R-Ras. *Cell* **85**, 61–69
 34. Pfaff, M., Liu, S., Erle, D. J., and Ginsberg, M. H. (1998) Integrin β cytoplasmic domains differentially bind to cytoskeletal proteins. *J. Biol. Chem.* **273**, 6104–6109
 35. Lad, Y., Harburger, D. S., and Calderwood, D. A. (2007) Integrin cytoskeletal interactions. *Methods Enzymol.* **426**, 69–84
 36. Smith, D. B., Berger, L. C., and Wildeman, A. G. (1993) Modified glutathione *S*-transferase fusion proteins for simplified analysis of protein-protein interactions. *Nucleic Acids Res.* **21**, 359–360
 37. Smith, D. B., and Corcoran, L. M. (2001) Expression and purification of glutathione-*S*-transferase fusion proteins. *Current Protocols in Molecular Biology* **28**:16.7.1–16.7.7
 38. Pearson, G., Bumeister, R., Henry, D. O., Cobb, M. H., and White, M. A. (2000) Uncoupling Raf1 from MEK1/2 impairs only a subset of cellular responses to Raf activation. *J. Biol. Chem.* **275**, 37303–37306
 39. Huttenlocher, A., Ginsberg, M. H., and Horwitz, A. F. (1996) Modulation of cell migration by integrin-mediated cytoskeletal linkages and ligand-binding affinity. *J. Cell Biol.* **134**, 1551–1562
 40. Liu, S., Calderwood, D. A., and Ginsberg, M. H. (2000) Integrin cytoplasmic domain-binding proteins. *J. Cell Sci.* **113**, 3563–3571
 41. Kato-Stankiewicz, J., Hakimi, I., Zhi, G., Zhang, J., Serebriiskii, I., Guo, L., Edamatsu, H., Koide, H., Menon, S., Eckl, R., Sakamuri, S., Lu, Y., Chen, Q. Z., Agarwal, S., Baumbach, W. R., Golemis, E. A., Tamanoi, F., and Khazak, V. (2002) Inhibitors of Ras/Raf-1 interaction identified by two-hybrid screening revert Ras-dependent transformation phenotypes in human cancer cells. *Proc. Natl. Acad. Sci. U.S.A.* **99**, 14398–14403
 42. Horwitz, A., Duggan, K., Buck, C., Beckerle, M. C., and Burridge, K. (1986) Interaction of plasma membrane fibronectin receptor with talin. A transmembrane linkage. *Nature* **320**, 531–533
 43. Franco, S. J., Rodgers, M. A., Perrin, B. J., Han, J., Bennin, D. A., Critchley, D. R., and Huttenlocher, A. (2004) Calpain-mediated proteolysis of talin regulates adhesion dynamics. *Nat. Cell Biol.* **6**, 977–983
 44. Franco, S. J., and Huttenlocher, A. (2005) Regulating cell migration. Calpains make the cut. *J. Cell Sci.* **118**, 3829–3838
 45. Yan, B., Calderwood, D. A., Yaspan, B., and Ginsberg, M. H. (2001) Calpain cleavage promotes talin binding to the $\beta 3$ integrin cytoplasmic domain. *J. Biol. Chem.* **276**, 28164–28170
 46. Woo, M. S., Ohta, Y., Rabinovitz, I., Stossel, T. P., and Blenis, J. (2004) Ribosomal S6 kinase (RSK) regulates phosphorylation of filamin A on an important regulatory site. *Mol. Cell Biol.* **24**, 3025–3035
 47. Ohta, Y., and Hartwig, J. H. (1996) Phosphorylation of actin-binding protein 280 by growth factors is mediated by p90 ribosomal protein S6 kinase. *J. Biol. Chem.* **271**, 11858–11864
 48. Kang, S., Dong, S., Guo, A., Ruan, H., Lonial, S., Khoury, H. J., Gu, T. L., and Chen, J. (2008) Epidermal growth factor stimulates RSK2 activation through activation of the MEK/ERK pathway and src-dependent tyrosine phosphorylation of RSK2 at Tyr-529. *J. Biol. Chem.* **283**, 4652–4657
 49. Kiema, T., Lad, Y., Jiang, P., Oxley, C. L., Baldassarre, M., Wegener, K. L., Campbell, I. D., Ylänne, J., and Calderwood, D. A. (2006) The molecular basis of filamin binding to integrins and competition with talin. *Mol. Cell* **21**, 337–347
 50. Vaidyanathan, H., and Ramos, J. W. (2003) RSK2 activity is regulated by its interaction with PEA-15. *J. Biol. Chem.* **278**, 32367–32372
 51. Renault-Mihara, F., Beuvon, F., Iturriz, X., Canton, B., De Bouard, S., Léonard, N., Mouhamad, S., Sharif, A., Ramos, J. W., Junier, M. P., and Chneiweiss, H. (2006) Phosphoprotein enriched in astrocytes. 15 kDa expression inhibits astrocyte migration by a protein kinase C δ -dependent mechanism. *Mol. Biol. Cell* **17**, 5141–5152
 52. Glading, A., Koziol, J. A., Krueger, J., and Ginsberg, M. H. (2007) PEA-15 inhibits tumor cell invasion by binding to extracellular signal-regulated kinase 1/2. *Cancer Res.* **67**, 1536–1544
 53. Belkin, A. M., Retta, S. F., Pletjushkina, O. Y., Balzac, F., Silengo, L., Fassler, R., Koteliensky, V. E., Burridge, K., and Tarone, G. (1997) Muscle $\beta 1D$ integrin reinforces the cytoskeleton-matrix link. Modulation of integrin adhesive function by alternative splicing. *J. Cell Biol.* **139**, 1583–1595
 54. Jockusch, B. M., Bubeck, P., Giehl, K., Kroemker, M., Moschner, J., Rothkegel, M., Rüdiger, M., Schlüter, K., Stanke, G., and Winkler, J. (1995) The molecular architecture of focal adhesions. *Annu. Rev. Cell Dev. Biol.* **11**, 379–416
 55. Beckerle, M. C., Miller, D. E., Bertagnolli, M. E., and Locke, S. J. (1989) Activation-dependent redistribution of the adhesion plaque protein, talin, in intact human platelets. *J. Cell Biol.* **109**, 3333–3346
 56. Bertagnolli, M. E., Locke, S. J., Hensler, M. E., Bray, P. F., and Beckerle, M. C. (1993) Talin distribution and phosphorylation in thrombin-activated platelets. *J. Cell Sci.* **106**, 1189–1199